Department of Meteorology
The University of Wisconsin
1 May 1965

NASw-65

AN INFLIGHT RE-CALIBRATION OF CHANNEL 3 ON TIROS IV

T. H. Vonder Haar, Inge Dirmhirn, and V. E. Suomi

The research in this document has been sponsored by the Division of Aeronomy and Meteorology, National Aeronautics and Space Administration under Contract NASw-65.

AN IN-FLIGHT "RE-CALIBRATION" OF CHANNEL 3 ON TIROS IV

FINAL REPORT

BY

T. H. VONDER HAAR, INGE DIRMHIRN, AND V. E. SUOMI

ABSTRACT

The reflected shortwave radiation sensor of the scanning radiometer on TIROS IV (Channel 3) degraded after launch. The amount of degradation is determined by comparing measurements of this medium resolution instrument with those from the University of Wisconsin omnidirectional sensor on the same satellite. This study accounts for the difference in resolution of the two radiometers. More than twenty comparisons were made at different times during the useful life of TIROS IV. The results show that besides a scale correction an additional intensity-dependent factor must be applied to Channel 3 values. This extra term is necessary to correct for electronic degradation and the wavelength-dependency of reflected radiation. Degradation apparently ceases after orbit 650, where the magnitude of the correction factor is near 2.0. These corrections bring the quasi-global summaries of measured albedo to a reasonable value of 33%.

I. INTRODUCTION

All channels of the scanning radiometer on TIROS IV, especially those designed to measure the reflected solar radiation from the earth, suffered an apparent drift of calibration. This "degradation" is discussed in the TIROS Manuals (1) and (2) and by Fritz, Rao, and Weinstein (3).

The TIROS 5-channel radiometers are calibrated before launch. The method of this calibration is described by Nordberg (4), Roche, et. al. (5), and, more in detail for a specific instrument, by Bartman, Surh, and Whybra (6). After launch there is no way to check the accuracy of these sensors directly.

The University of Wisconsin's hemispheric radiation sensors were also flown on TIROS IV. These instruments can be calibrated in flight as they warm and cool leaving or entering the earth's shadow. Data obtained from the scanning radiometer can be compared with measurements of this omnidirectional sensor over the same region. Thus a correction factor for degradation can be established for the readings of the scanning radiometer. Since comparisons can be made at different orbits, the change of this factor during the lifetime of the satellite can be obtained.

This study specifically deals with the correction of Channel 3 (0.2 ------- 6.0 microns) on TIROS IV. We want to examine the response of this sensor at <u>definite points in space and time</u> and over a variety of meteorological conditions. Since the resolution of the scanning radio-

meter is quite good, its data, if accurate, could be usefully applied to the investigation of many meteorologically important situations. Two attempts have already been made to correct these data. They are discussed in the TIROS IV User's Manual (2) and briefly described below.

One method used quasi-global averages of both long and shortwave radiation reported by the scanning radiometer, together with the results of a theoretical heat balance study, in an attempt to measure degradation. This approach assumes that both the theoretical study and the measured longwave values are accurate. In addition, such a large amount of averaging could possibly conceal significant characteristics of the degradation. Correction factors obtained in this manner can be applied confidently to all data only if it can be assumed that the sensor responds equally over its entire range.

A second attempt consisted of flying a balloon-borne TIROS instrument package under a satellite pass. The difference in elevation of two instruments with the same aperture angle caused each instrument to view different portions of the earth's surface. With a uniform reflectance over a large area one could assume similar conditions for both instruments. Unfortunately, the meteorological conditions were not favorable at that time (scattered clouds were present), and thus the comparison contains some uncertainty. Even if this difficulty could be overcome, the resulting measure of degradation would hold for only a single instant of the satellite's useful life.

A third technique has been considered by several investigators. They propose to compare individual measurements of the beam radiometer with "standard" albedoes determined by theoretical studies or aircraft measurements. Such a comparison is difficult because of errors arising from:

1) positioning of the satellite measurement
2) fluctuations of the radiometer housing temperature
3) noise in the satellite data
4) erratic shifts of the zero level
5) wavelength-dependency of reflected radiation
6) angular dependence of reflected radiation
7) non-uniformity of the viewed surface
8) uncertainty of the standard used for comparison
9) time differences

It is apparent that Channel 3 data have not been accurately corrected. The method presented here, a direct comparison of two instruments in flight, should produce an accurate determination of Channel 3 degradation. Furthermore, it should provide some information about the type of degradation that occurred.

II. CRITERIA OF THE COMPARISON

The characteristics of the two instruments under consideration have been discussed in detail by Bandeen, et. al. (7), and in the TIROS Manuals (1) and (2) for the scanning radiometer; by Suomi (8), House (9), and Sparkman (10) for the omnidirectional radiometer.

To compare two solar radiation sensors on the same satellite the following points must be considered:

a) difference in spectral response
b) difference in resolution
c) difference in the accuracy of the telemetry system

a) A mirror, filter and sensor device provides Channel 3 with a spectral response from 0.2 - 6 microns, as shown in Figure 1. The dip in the curve between 0.6 and 1 micron is due to the reflection loss of an aluminum mirror. There exists a decrease of sensitivity toward the shortwave end of the spectrum.

The omnidirectional instrument employed the temperature difference between a black and an aluminum coated sensor to determine the shortwave radiation. This device gave a fairly even reflectance over the whole spectrum in question.

b) The area on the earth's surface from which each sensor obtains a single measurement of energy is not the same. Suomi (8), Bignell (11), and House (9) have described the geometry necessary to determine the area viewed by the low resolution instrument. This sensor's view extends from horizon to horizon and depends only on the satellite's height. For the mean TIROS IV satellite height of 750 km. the diameter

of the total field of view is 53° of geographical latitude. Fifty and eighty per cent of the energy measured is obtained from circular areas with diameters of 13.5° and 24° of latitude respectively.

The medium resolution instrument is constructed to scan the earth and collect radiation measurements from individual scan spots along a scan line. The area of the earth viewed by each scan spot varies considerably with sensor nadir angle. A complete treatment of the geometry has been given by Fujita (12). Using his values of aperture angle versus relative sensitivity, computations of the relative power versus view angle were carried out and are shown in Figure 2. Using the results shown in this figure we can calculate the approximate areas viewed at 100% power (8° aperture angle) for different nadir angles, as shown in Figure 3. Thus, one can see that the size of this area, or scan spot, can vary considerably with satellite nadir angle.

A scan line consists of the narrow arc traced across the earth's surface by the sensor as the satellite spins. Motion of the satellite along its orbit advances the scan lines. The satellite spins at a mean rate of 10 rpm and a typical open single mode scan line, 2,500 km. long, contains approximately 25 scan spots. In the closed mode the number of scan spots increases to about 40, while at the beginning of the alternating mode a scan line only consists of approximately 10 scan spots. Of these readings only the first horizon and each fifth value thereafter are read directly from the analog records. All other scan spot radiation values are interpolated. An example of the power areas of selected

scan spots on consecutive scan lines is given in Figure 4. It is apparent that use of all scan spots on every scan line enables the medium resolution radiometer to view nearly the entire area under the satellite pass.

To perform a valid comparison we must overcome the difference in resolution and force each sensor to "see" the same area. Thus it is necessary to integrate many single measurements of the scanning radiometer and to compare the result with one reading of the low resolution instrument over the same area.

c) The telemetry system is the same for both instruments. To avoid errors caused by a low signal - to - noise ratio, comparisons were made over regions with the highest solar zenigh angles (i.e., near the equator).

The equatorial cases chosen to satisfy the above requirement posed an additional problem in selecting cases for study. At the equator the distance between two consecutive satellite tracks is a maximum. The medium resolution instrument views equal areas on either side of the track only when the departure of the satellite spin axis from the orbital plane is a minimum. This angle of departure, the "minimum nadir angle," varies with the orbit number. Near the equator, scanning radiometer data from three consecutive passes of TIROS IV cover the area viewed by the low resolution sensor only if the minimum nadir angle is less than 10^{o}. The scan lines are then relatively symmetrical about the sub-satellite track, and so few data gaps occur.

The requirements of high sun angle and good coverage considerably limit the situations where a valid comparison can be made. Figure 5 shows that comparisons were possible in short periods during all months while the satellite was in orbit.

At this point we have defined the conditions under which a comparison must be made. In discussing the mechanics of our method, the following factors must be considered:

a) The comparison must be made over equatorial regions.

b) It must be made when the satellite's attitude permits both sensors to view the same area.

III. METHOD OF COMPARISON

A value of reflected shortwave 4adiation is measured by the low resolution sensor at a given time and geographical location. The relation between this value from the omnidirectional hemispheric sensor and the many measurements taken by the medium resolution scanning radiometer over the same area was determined by a simple numerical integration.

Where:

$$F = \int_0^{2\pi} \int_0^{\pi/2} I \sin\theta \, d\theta \, d\phi \qquad (1)$$

$$F' = \int_{\pi/N}^{\pi/N+1} \int_{\pi/M}^{\pi/M+1} I \sin\theta \, d\theta \, d\phi \qquad (2)$$

$$F = \sum_{N=0}^{N=2\pi} \sum_{M=0}^{M=\pi/2} (F') \qquad (3)$$

and:

F = total flux of radiation

F'= the contribution to the total flux by an incremental area of the hemisphere

For this study ten concentric circles around the subsatellite point were determined. From each of these ring-areas the low resolution sensor receives 10% of the total reflected energy measured, (House (13)). The shortwave radiation measurements from the medium resolution instrument are assigned to one of these weighting areas on the basis of an adjusted sensor nadir angle. This angle is obtained

by relating the position of each scan spot to the satellite's position at the time of the low resolution measurement. The exact geographical location of the scan spots remains unchanged. One of the cases chosen is shown in Figure 6. A few distorted scan lines, described by Davis (14), are apparent in the lower right-hand portion of the figure. It is possible to correct these misplaced scan spots. Since this extensive process would seldom position a spot in a different weighting area, we did not correct the location of these points.

Because portions of three orbits of scanning radiometer data were used to provide adequate coverage, a simple correction for the 100 minute time difference with respect to the central pass was necessary. The pattern of cloud cover was assumed not to vary over this time period. Then each contributing scan spot needed only to be corrected for the change in sun angle. The above-mentioned choice of cases occurring near local noon minimized the change in cosine law of incident radiation and therefore the correction.

The low resolution sensor integrates into its total value the effect of limb-brightening. If we assume that this effect occurs all along the horizon, we must account for a similar occurrence at high sensor nadir angles of the medium resolution instrument (i.e. near the extremities of scan lines traced by the scanning radiometer). A simple calculation shows that the measurement of the low resolution instrument includes a limb-brightening of π times the diameter of the area in question, while the brightening effect along the traces of the scanning radiometer are of a length slightly less than four times

the diameter. Exact measured lengths show 12% more limb-brightening areas for the scanning radiometer than for the hemispheric instrument. These values are valid only for the assumption of a limb-brightening effect all around the horizon. Obviously limb-brightening will be at a minimum near local noon.

The data gaps mentioned in the previous section occur when the medium resolution sensor does not obtain measurements for a portion of the total area viewed by the low resolution sensor. Even when the minimum nadir angle is within the required limits, gaps can occur if the scanning radiometer is sampling in the closed mode configuration. Primarily for this reason, use of closed mode data was avoided as much as possible. The error introduced into the comparisons by the few gaps that do occur is very small because the number of scan spots considered is large enough to assure a statistically acceptable value (see Table 1). If the meteorological conditions are fairly uniform over the total area considered, no error is caused by a gap.

TABLE I

NUMBER OF SCAN SPOTS IN WEIGHTING AREAS

WEIGHTING AREA	1	2	3	4	5	6	7	8	9	10
NUMBER OF SCAN SPOTS	66	79	111	114	182	245	274	399	892	7054

(This example of the number of scan spots is taken from orbit No. 736, with a height of the satellite of 721 km. The numbers vary slightly with height and from one case to the other. For our comparison, the values in Table I can be taken as an average case).

As a result of the unique method of inflight calibration and resulting reduction of low resolution measurements, actual values of albedo were used from that sensor. For any fixed point and time the relat on between this accurate albedo measurement and the appropriate weighted average of the reflected shortwave scanning radiometer is:

$$A = \frac{SW\uparrow}{\left(\frac{2.0}{K}\right)\cos\zeta_{\odot}} = D\overline{W}'/\bar{\phi}\,C\left(\frac{2.0}{K}\right)\cos\zeta_{\odot} \qquad (4)$$

Where:

A = albedo of area viewed (%)

SW↑ = accurate value of reflected shortwave radiation (ly/min.)

K = correction to solar constant for earth-sun distance (Solar constant is assumed equal to 2.00 ly/min.)

$\zeta_{\odot}$ = zenith angle of sun

$\bar{\phi}$ = mean spectral response of Channel 3 = 0.53

C = conversion factor relating watts/m^2 to ly/min. = 698.17

W'= weighted area average of reflected shortwave radiation as measured by Channel 3 (watts/m^2)

D = the correction factor

IV. RESULTS

A correction factor, D, derived from Equation (4), was computed for all situations satisfying the requirements for a comparison. The results of three such cases are shown in Table (2). Each case consists of comparisons made at five consecutive low resolution sensor measurements. There is a 30 second time interval between each comparison on the same orbit. This corresponds to a 75 nautical mile displacement of the subsatellite point along the orbit t5ack. The measured value of omnidirectional sensor albedo describes the type of reflecting surface (i.e., cloud cover and/or surface terrain). The observed magnitude of degradation changes very little with time if the reflecting surface is nearly the same. Within the same orbit or between adjacent orbits, however, the value of D varies considerably if meteorological conditions change.

The weighted average of values measured by Channel 3, $\overline{W}'$, also gives a gross relative estimate of the type of reflecting surface in view. In Figure (7) the variation of D with $\overline{W}'$ is presented for each of the time periods where comparisons were possible (i.e., near orbits 90, 650, 730, 1120, and 1600). It is apparent that both the magnitude of the derived correction factor, and its variation with the measured average intensity, is nearly the same for all time periods after orbit 650. Only two situations near orbit 90 fulfilled the requirements of a comparison, and both had similar meteorological conditions. The

magnitude of Channel 3 degradation detected near orbit 90 is less than that detected for later orbits. Figure (8) is a least squares fit of D and $\overline{W}'$ for all comparisons performed past orbit 650.

The results of our inflight comparisons of Channel 3 with the omnidirectional sensor indicate rapid post-launch degradation of Channel 3. This degradation apparently ceases after orbit 650. Furthermore, our results show a need to increase the correction factor as the reported Channel 3 intensity decreases.

TABLE (2)

ORBIT	LAT.	LONG.	ALBEDO	$\bar{W}'$	D
	-0.2	153.4E	.38	127.82	2.24
	1.1	154.4	.37	122.71	2.26
697	2.5	155.5	.36	116.82	2.27
	3.8	156.5	.35	113.43	2.29
	5.1	157.6	.34	112.67	2.30
	12.4	35.5E	.35	109.50	2.25
	11.1	36.6	.35	110.04	2.25
1119	9.8	37.7	.35	111.03	2.25
	8.5	38.7	.35	111.68	2.26
	7.2	39.8	.345	111.20	2.27
	12.3	61.0E	.175	42.30	2.71
1118	11.0	62.1	.185	47.19	2.69
	9.7	63.1	.195	51.23	2.68
	8.4	64.2	.21	56.72	2.66
	7.1	65.3	.22	60.82	2.64

V. DISCUSSION OF RESULTS

The degradation of the TIROS scanning radiometer sensors has never been fully understood. Bandeen, et. al. (1) have discussed possible kinds of degradation in considerable detail. There are two basic types: (a) uniform (symmetrical) degradation, where the response of a sensor decreases to some fraction of its pre-launch value; and (b) non-uniform degradation, where a sensor's response is energy-dependent. The uniform type is most apparent (i.e. when the mean quasi-global albedo is reported as 15 %), but probably least understood. Non-uniform degradation can be caused by several factors, and affects a sensor's accuracy primarily at the low range of intensities. Electronic degradation (characterized by a shift in the space-viewed (zero) level) is an example of this kind of degradation. Since pre-launch determined calibration curves are used to reduce all scanning-radiometer data, the magnitude and direction of a zero shift with respect to the pre-launch zero must be considered. In such a case, an energy-dependent correction factor must be applied to the reduced data, in addition to the correction for uniform degradation, if it occurs. Post-launch theoretical and laboratory examination of reduced data can detect both types of degradation. The accuracy of such investigations is limited by the theory and techniques that can be applied.

An inflight degradation check should detect both types of degradation if they exist. Our results show that the response of

Channel 3 is definitely energy-dependent. The magnitude of the non-uniform component is not readily apparent since we measure only total degradation. Our results do indicate that the direction of this component implies a downward shift of the space-viewed level, or some analogous effect, or both.

Since our comparisons show that two types of degradation affected Channel 3 on TIROS IV, let us now theoretically examine the data and techniques we have used, in an attempt to physically substantiate our results. We will borrow the notation devised by the NASA Staff Member's (15) in their treatment of TIROS VII data. Where:

$$\overline{W} = K\,(\,\overline{W}' + \rho\,) \qquad (5)$$

$\overline{W}$ = true value of Channel 3 intensity corrected for all degradation

K = correction factor for uniform degradation

$\overline{W}'$ = uncorrected intensity measurement

$\rho = \sum \rho_i$ = total of all adjustments necessary to correct for non-uniform degradation (watts /m^2)

and:

$$\rho_i = \frac{(\,-\Delta F_i\,)}{dF}\, d\overline{W}' \qquad (6)$$

where:

i = subscript that identifies the process necessitating the adjustment

ΔF_i = real or simulated shift in the space-viewed level caused by the process " i " (c.p.s.)

$dF/d\overline{W}' = 0.1125$ = idealized linear transfer function arising from the pre-launch calibration (c.p.s. / watts $\cdot$ m^{-2})

We will first look for evidence of non-uniform degradation, described by the parameter, p. The magnitude of p will determine how much any uncorrected Channel 3 measurement should be adjusted before a correction for uniform degradation is applied. Its value could result from the action of one or more processes. According to our results, such processes must cause or simulate a negative ΔF. They must force the sensor to yield a more accurate measurement over regions of greater reflectance. It is also possible that some factor peculiar to our comparison has simulated the observed non-uniform effect. We will consider:

a) the omni-directional sensor data used

b) the scanning radiometer data used

c) the method of comparison

d) the electronics of Channel 3

e) the spectral response of Channel 3

a) The albedo values of the low resolution sensor are the foundation for our comparison. If the lag of this sensor's response was not correctly applied in obtaining albedo values, a simulated zero shift downward could occur. Such an effect would be evidenced by an anomolous dependence of the correction factor on energy for comparisons made when the hemispheric sensor's temperatures were rising. This did not occur. A signal from a reference thermistor in the hemispheric sensor package was found to change slightly over a long time period. Any variation was considered in obtaining albedo values, and therefore electronic degradation was removed. The effective zero level of the

low resolution sensor for albedo calculations is the temperature of the white hemisphere. The response of this component is checked twice each orbit as part of the inflight calibration procedure. Nothing in the observed behavior of this sensor indicates a shift in the zero level. Thus, the observed energy-dependent correction factor does not result from a property of the low resolution sensor.

b) Most errors associated with reducing the scanning radiometer data would have a random effect on our comparison. However, the five-channel instrument is sensitive to changes in the temperature of the radiometer housing, T_c. Mean values of T_c over an orbit were used by NASA to reduce the scanning radiometer data. All of our comparisons were made near local noon. Minimum values of T_c are observed after the satellite enters the sunlight portion of an orbit. All comparisons are then made when the housing temperature is less than the mean. Prelaunch calibration showed that Channel 3's zero level is proportional to T_c. A downward shift of the space-viewed level is therefore simulated by the effect of radiometer housing temperature on our comparison. Assuming our comparisons are made at a T_c which is 1.5° C. less than the mean value, it was found that the value $\overline{W}'$ used to compute all inflight determined correction factors should be increased by 3 W/m^2. This correction was applied in Figure (8). The result, the dashed line, represents the energy-dependent correction factor from which all bias due to the housing temperature effect has been removed.

c) All comparisons were divided into groups having the same values of dip angle, solar zenith angle, etc. In every subdivision the dependence of correction factor on intensity was present.

d) Δ F for Channel 3 of TIROS IV was determined at NASA by qualitative examination of the analog records. An independent check was performed at the University of Wisconsin, in cooperation with the Electrical Engineering section of this project. The results are nearly the same and are shown in Figure (9). A mean value of ΔF = -5cps was found. From Equation (6), the adjustment for electronic degradation, p_e, equals 4.5 w/m^2. The accuracy of both methods for determining ΔF suffers due to noise in the signal.

e) The response of Channel 3 is slightly wavelength-dependent. Careful examination of the sensor's relative spectral response in Figure (1) shows that for wavelengths less than 8000 Å the value is 0.49. In the wavelength interval 8000 - 40,000 Å it is 0.57. A mean spectral response of 0.53 was used in deriving D. Thus, the sensor responds better than the mean to reflected radiation outside the ultra-violet and visible region. This fact would be insignificant if all sampled conditions scattered radiation equally for all wavelengths. Incident solar radiation is not scattered uniformly with wavelength under certain conditions. Scattering by air molecules is extremely selective ($\sim 1/\lambda^4$). Forty-five per cent of the incident solar energy is at wavelengths greater than 8000 Å, but a clear sky scatters only about 1% of this amount. For a case of clear sky over the ocean (a region of low reflected intensity) Channel 3 measures energy primarily at wavelengths where it is least accurate. Scattering by large particles is less selective. For a case of measured high reflectance over an overcast region the sensor measures nearly a full

spectrum of energy and its response is close to the mean value assumed. The non-uniform effect produced by this wavelength-dependency requires measurements to be adjusted by an effective p-value, p_λ . The value of this adjustment is 4.5 w/m^2; it is equivalent to $\Delta F = -0.5$ cps.

The value, p_λ , does not represent degradation. It arises from the combination of an instrumental characteristic with physical scattering processes. Calibrating Channel 3 is most difficult at shorter wavelengths (Roche, et. al. (5)). Continuous exposure to a space environment could cause non-uniform degradation of the sensor. These factors could increase or slightly diminish the magnitude of p_λ .

The results of our comparisons have served to indicate the existence of non-uniform degradation. An investigation, independent of the comparison, found that the magnitude of this component can be equivalent to $p \approx 10$ watts/m^2, or $\Delta F = -1.0$ cps. The processes contributing to this effect are:

	p (watts/m^2)	ΔF (cps)
Electronic degradation	4.5	-0.5
Wavelength-dependency	4.5+	-0.5 (simulated)
Total	$\approx$ 10	-1.0

The remaining parameter describing degradation, K, can now be determined by again applying the technique used by NASA for TIROS VII. With:

$$A = \overline{W}' \,/\, \overline{W}^* \cos \zeta_\odot \qquad (7)$$

and Equation (5) we have:

$$K = \left[\frac{A}{A' - \left(\frac{\Delta F}{K \overline{W}^* \cos \zeta_\odot} \right)} \right] \qquad (8)$$

Where:

A = diffuse albedo corrected for all degradation

A'= uncorrected diffuse albedo

$\overline{W}^*$= 739 w/m^2 for 1 solar constant radiated from a diffuse source (see Appendix I)

$k = dF / d\overline{W}'$

For orbits past 650, "normalizing" Channel 3 quasi-global albedoes to those of the omnidirectional sensor requires A' = 15.5 % and A = 32 %. Assuming the mean value of $\cos\ell_o$ = 0.827 we have, with F = -1.0 cps, $\underline{K = 2.05}$

Since: $\overline{W} = \overline{W}'D_T$ where (9)

D_T= theoretically determined correction for total degradation

From (5) and (9)

$$D_T\overline{W}' = K (\overline{W}' + p)$$

or $$D_T = K (1 + p/\overline{W}')$$

With the values of p and K already known we can compute D_T and compare with D, the correction factor for total degradation determined by our comparisons (dashed line in Figure 8).

For example:	$\overline{W}'$	D_T	D
	50	2.46	2.46
	100	2.25	2.27

The factors determined theoretically and those resulting from inflight comparisons agree very well. This means the observed non-uniform degradation can be explained by the two processes discussed above, electronic degradation and wavelength-dependency.

With the values of ρ and K fixed we can also use Equation (11) to find D, the total correction factor, for intensities outside the range of those used in the comparisons. As shown in Figure (10), the effect of ρ decreases at higher intensities. Fortunately, most comparisons were made at relatively low values of $\overline{W}'$ where the non-uniform effect could be measured.

In Figure (11) the inflight derived correction factors are shown as a function of time and intensity. The value $\rho = p_e + p_\lambda$, found constant after orbit 650, is assumed valid for all orbits. The curve for $\overline{W}' > 300$ w/m^2 represents the variation of K with time. In the same figure, we have presented the correction factor determined by the NASA Staff Members (2). It is derived considering only uniform degradation. Its value, 1.97, (see Appendix I) was determined by the quasi-global average method, and agrees quite well with our results if non-uniform degradation is ignored. This agreement is made possible because the earth-atmosphere system was in a state of near-radiative equilibrium during the useful life of TIROS IV.

Initially, the correction factor determined by the balloon experiment was in agreement also. However, subsequent re-evaluations of the balloon results gave factors of 1.3 or 1.6. If these values are used the mean quasi-global albedo is 20% or 25%.

VI. ESTIMATE OF ACCURACY

Several factors that might influence the accuracy of our comparisons have been discussed in previous sections (i.e. limb-brightening, gaps in the scanning radiometer coverage, etc.). These effects are insignificant if cases for comparison are carefully chosen. Variations in the radiometer housing temperature, although considered, also have a small effect on our results.

Our observed variation of correction factor with intensity has been explained. The magnitudes of our correction factors are obviously dependent on the accuracy of the low resolution sensor albedo values we used. The Wisconsin hemispheric sensors are calibrated in flight. It is possible to observe the behavior of both the black and the white sensors before, during, and after the time that temperatures from these sensors are used to compute an albedo value. Based on such observations, we assign an absolute error of $\pm$ 3% to an <u>individual</u> low resolution sensor albedo value. (Note: the accuracy of averaged hemispheric sensor albedo values, especially those obtained from a technique using only the black sensor temperatures, is much better). Since the albedo calculation is essentially a difference technique, measurements over highly reflecting surfaces contain less error. In fact, this error is significant only for values of $\overline{W}'$ less than 50 w/m^2; where our correction factor can be in error by $\pm$ 0.4. Even so, a corrected reflectance would be within $\pm$ 3% of the true value.

In this study, we have assumed that solar radiation is reflected isotropically. For cloud and ocean surfaces, however, scattering is most pronounced in the forward direction. The selection of comparisons near local noon should minimize this effect. Caution should be used in applying our inflight derived correction factors to situations where specular reflection occurs.

Perhaps the best test of our results can be obtained by applying them to some typical Channel 3 measurements. Values of less than 10 w/m^2 have been reported by Channel 3 even with the solar zenith angle less than 30^o. These occur over the ocean under clear skies. On the other hand, Channel 3 measurements greater than 300 w/m^2 are quite rare, even at local noon.

In Table (3) the reflectances are shown that result from applying: no correction, a correction factor of 1.6, and our in-flight determined correction factor, D.

TABLE III

Condition	$\theta_\odot$	$\overline{W}'$	r'	$r_{1.6}$	r_D
Clear sky over ocean	30^o	10 w/m^2	.016	.025	.065
High cloud deck	0^o	300 w/m^2	.40	.63	.86

VII. CONCLUSION

Our inflight comparison of Channel 3 and the omnidirectional sensor on TIROS IV has provided accurate correction factors for Channel 3. Its data can now be more usefully applied.

The correction factor that should be applied to a Channel 3 measurement made during a certain orbit can be obtained from Figure (11) or computed from:

$$D = K \left(1 + {}^{10}/\overline{W}' \right)$$

Where K = 2.05 is constant after orbit 650. To obtain a corrected intensity or reflectance measurement use:

$$\overline{W} = D\overline{W}'$$

or

$$r = D\overline{W}'/739 \cos \zeta_{\odot}$$

The detection of non-uniform degradation in the response of Channel 3 lead to an investigation of that sensor's electronics and spectral response. Electronic degradation did occur. It was also found that under certain meteorological conditions the assumption of a mean spectral response is not valid. This fact might be important in other channels of the scanning radiometer.

Our comparison also demonstrated another advantage of including more than one radiation subsystem on meteorological satellites.

APPENDIX I

In the course of this study it was necessary to determine the mean spectral response of Channel 3, $\bar{\phi}$, which is used in Equation (4). Since: $\bar{\phi} = \int_0^\infty I_\lambda \phi_\lambda d\lambda \Big/ \int_0^\infty I_\lambda d\lambda$ a weighted integration using Figure (1) gave $\bar{\phi} = 0.53$. However, the constant $\bar{W}^*$ is defined as:

$$\bar{W}^* = \int_0^\infty S_\lambda \phi_\lambda d\lambda$$

Where: $\int_0^\infty S_\lambda d\lambda =$ the solar constant at 1 AU = 1395 watts/m^2, using $\bar{\phi} = 0.53$ yields $\bar{W}^* = 739$ watts/m^2, slightly larger than the value of 691 watts/m^2 quoted in the TIROS IV User's Manual. There are two results of this slight adjustment of Channel 3's mean spectral response:

a) a reflectance (diffuse albedo) value should be computed using $r = \bar{W}/739 \cos \zeta_\odot$

b) as a result of (a) the mean quasi-global albedoes reported in the TIROS IV User's Manual should be decreased about 1% . This small change, however, raises the correction factor determined by the quasi-global averaging method from 1.84 to 1.97.

This is a good example of the sensitivity of the scanning radiometer before any degradation is even considered. Such uncertainties hamper the accuracy of any check of degradation study.

REFERENCES

1. TIROS III Radiation Data User's Manual Supplement, Goddard Space Flight Center, Greenbelt, Dec. 1963.

2. TIROS IV Radiation Data Catalog and User's Manual, Goddard Space Flight Center, Greenbelt, Dec. 1963.

3. Fritz, S., K. Rao, and M. Weinstein, Satellite Measurements of Reflected Solar Energy and the Energy Received at the Ground. Journal of the Atmospheric Sciences, 21, March 1964.

4. Nordberg, W., Physical Measurements and Data Processing. Proceedings of the Int. Meteor. Sat. Workshop, Nov. 13-22, 1961, 107-119, Washington 1961.

5. Roche, J. J., Drummond, A. J., and D. T. Hilleary, Report on the Test and Calibration of a TIROS III FIVE-CHANNEL RADIOMETER, Contract CWB - 10075, The Eppley Laboratory, Inc., Newport, R. I., April 1964.

6. Bartman, F. L., M. T. Surh, and M. G. Whybra, Long - Term Integrity of the TIROS 5 - Channel Radiometer Visible Channel Characteristics, The Univ. of Michigan, NASA, Contract No. NASw - 140 Report, Dec. 1963.

7. Bandeen, W. R., R. A. Hanel, J. Licht, R. A. Stampfl, and W. G. Stroud, Infrared and Reflected Solar Radiation Measurements from the TIROS II Meteorological Satellite. Geophys. Res. 65, 3169 - 3185, 1961.

8. Suomi, V. E., The Thermal Radiation Balance on Board EXPLORER VII, NASA Technical Note D-608, July 1961.

   Suomi, V. E., I. G. Y. Annals, 1959, 331 - 340.

9. House, J. B., The Earth's Radiative Balance from a Satellite. Ph.D. Thesis, Univ. of Wisconsin, 1965.

10. Sparkman, Barbara B., Experimental Analysis of the TIROS Hemispheric Sensor, M.S. Thesis, Univ. of Wisconsin, 1964.

11. Bignell, K. J., Heat Balance Measurements from an Earth Satellite - an Analysis of Some Possibilities, Quarterly Journal of the Roy. Met. Soc., 231 - 244, 1960.

12. Fujita, T., Outline of a Theory and Examples for Precise Analysis of Satellite Radiation Data, Mesomet. Proj. Res. Paper No. 15, Univ. of Chicago, Feb. 1963.

13. House, F. B., On the Interpretation of Longwave Radiation Data from EXPLORER VII Satellite, Progress Report No. 1, 1963.

14. Davis, P. A., Satellite Radiation Measurements and the Atmospheric Heat Balance, Final Report, Contract NAS 5-2919, Goddard Space Flight Center, Greenbelt, Md.

15. TIROS VII Radiation Data Catalog and User's Manual, Vol. 1, Goddard Space Flight Center, Greenbelt, Maryland, Sept. 1964.

LIST OF FIGURES

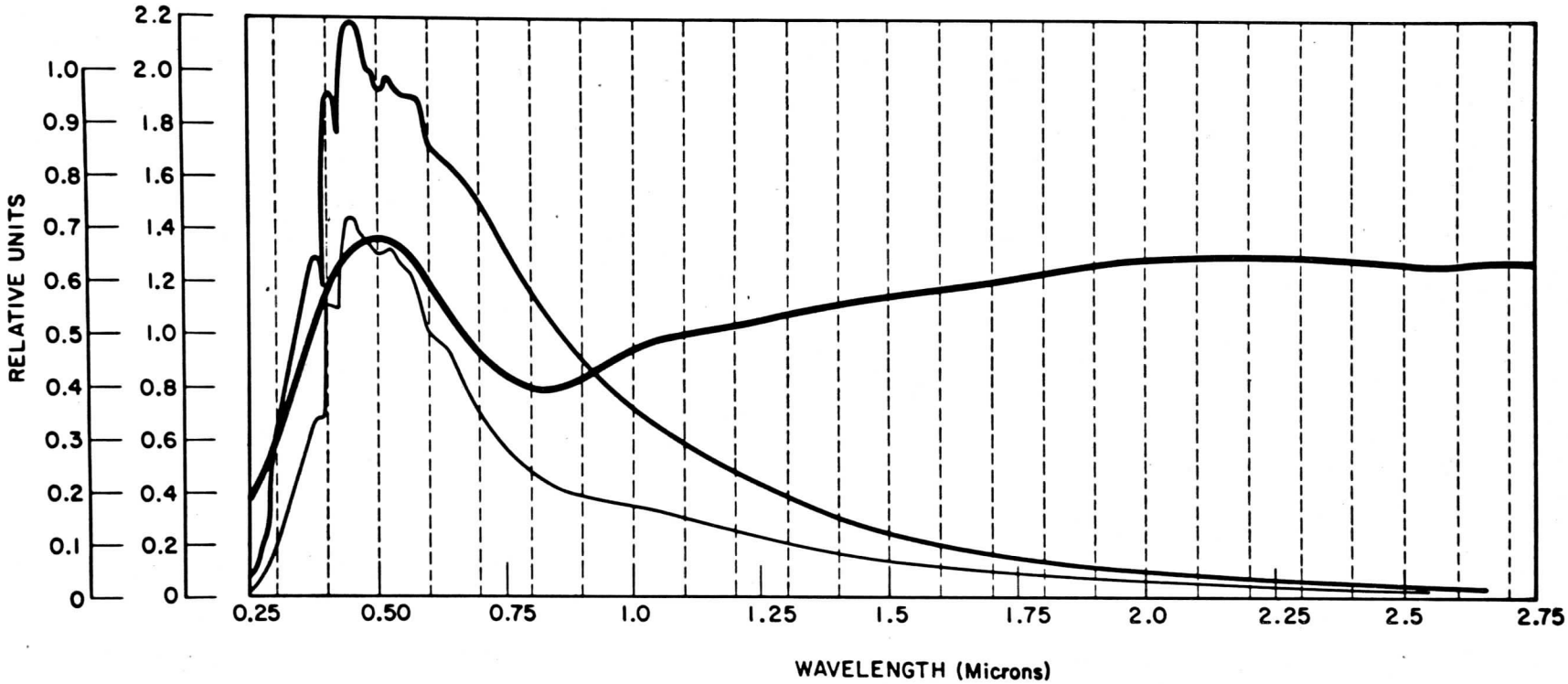
RELATIVE UNITS
1.0
0.9
0.8
0.7
0.6
0.5
0.4
0.3
0.2
0.1
0
2.2
2.0
1.8
1.6
1.4
1.2
1.0
0.8
0.6
0.4
0.2
0
0.25
0.50
0.75
1.0
1.25
1.5
1.75
2.0
2.25
2.5
2.75
WAVELENGTH (Microns)

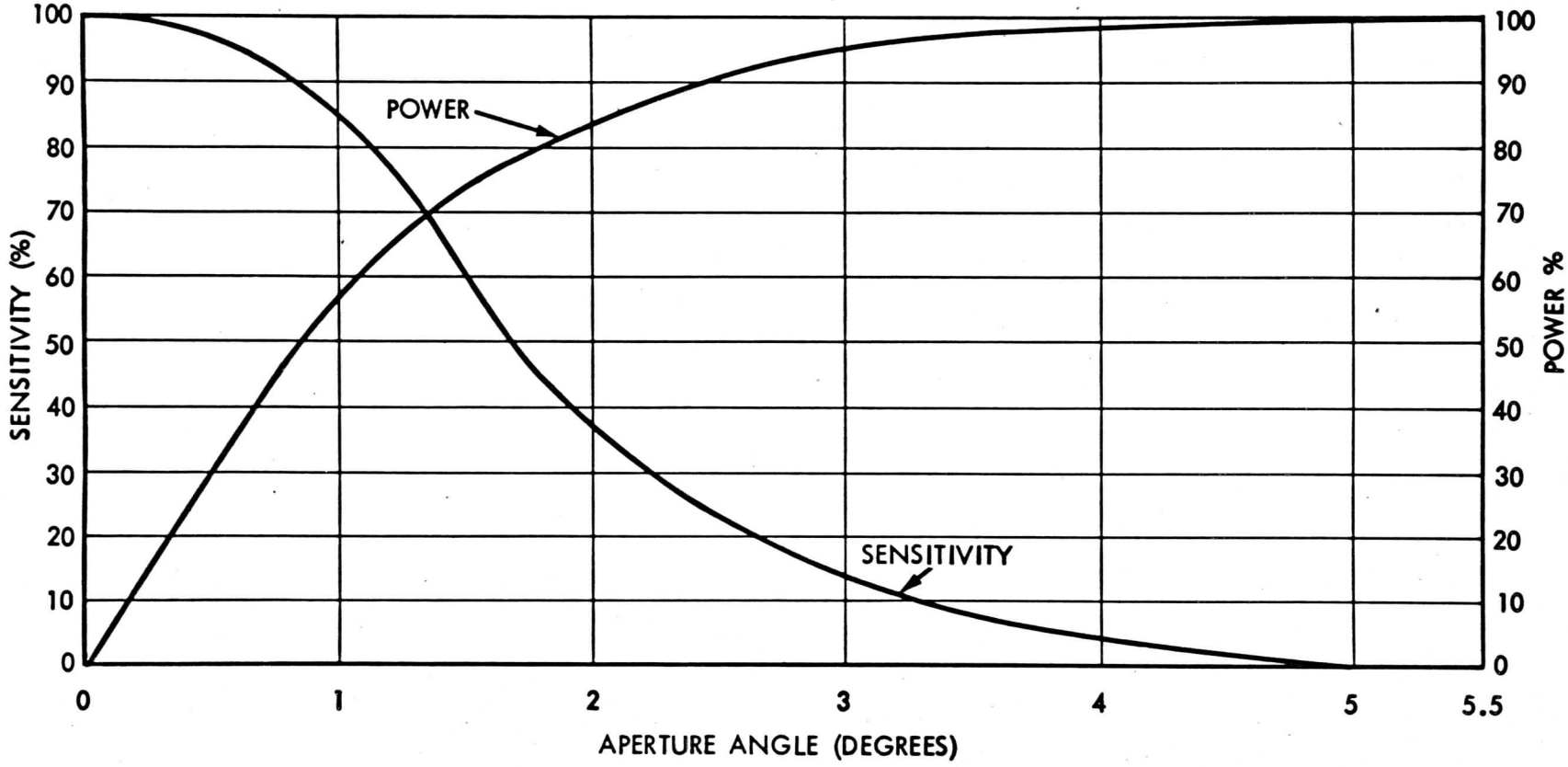
100
90
80
70
60
50
40
30
20
10
0
SENSITIVITY (%)
POWER
SENSITIVITY
POWER %
0
1
2
3
4
5
5.5
APERTURE ANGLE (DEGREES)

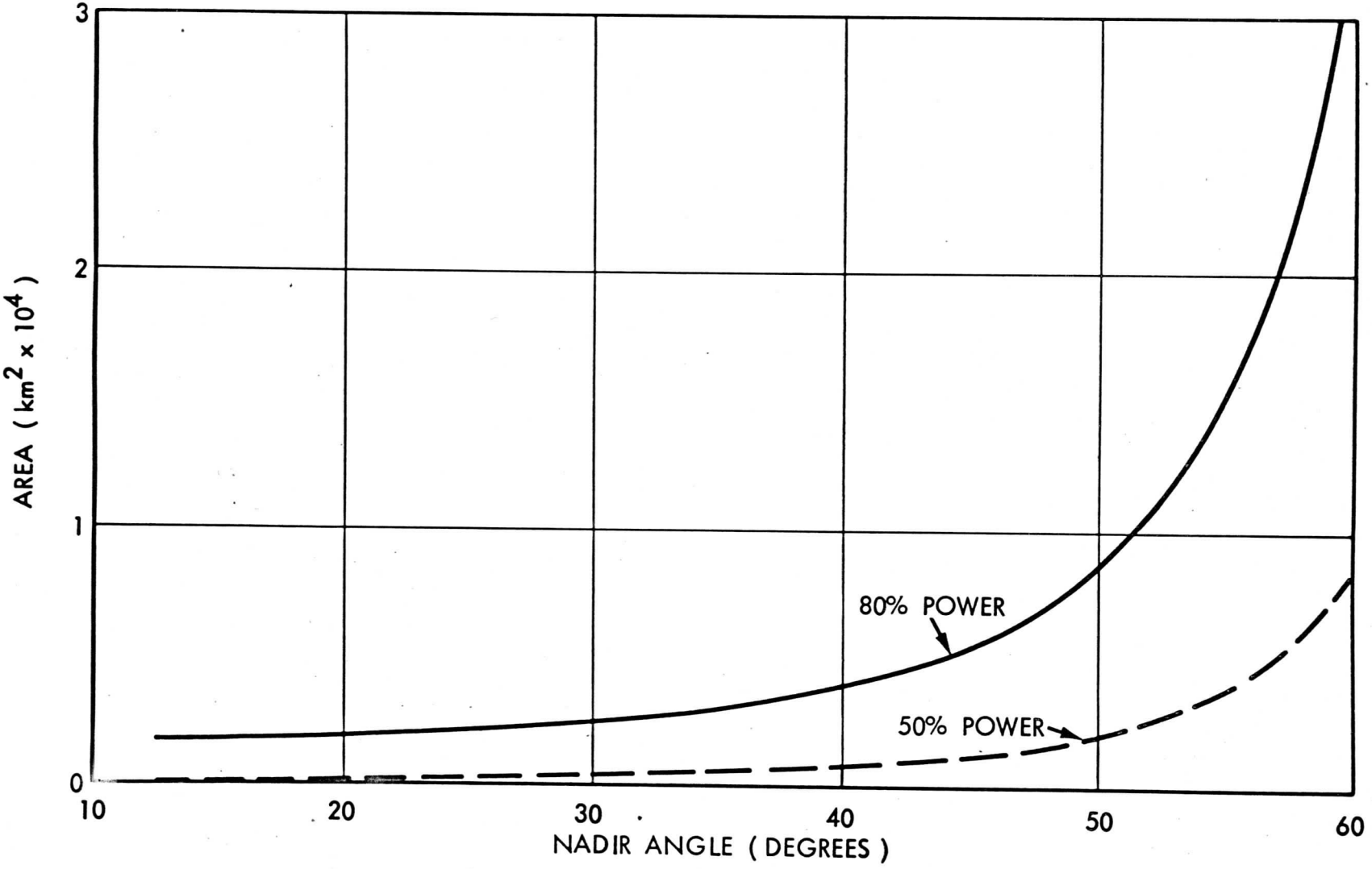
AREA (km² x 10⁴)
3
2
1
0
10
20
30
40
50
60
NADIR ANGLE (DEGREES)
80% POWER
50% POWER

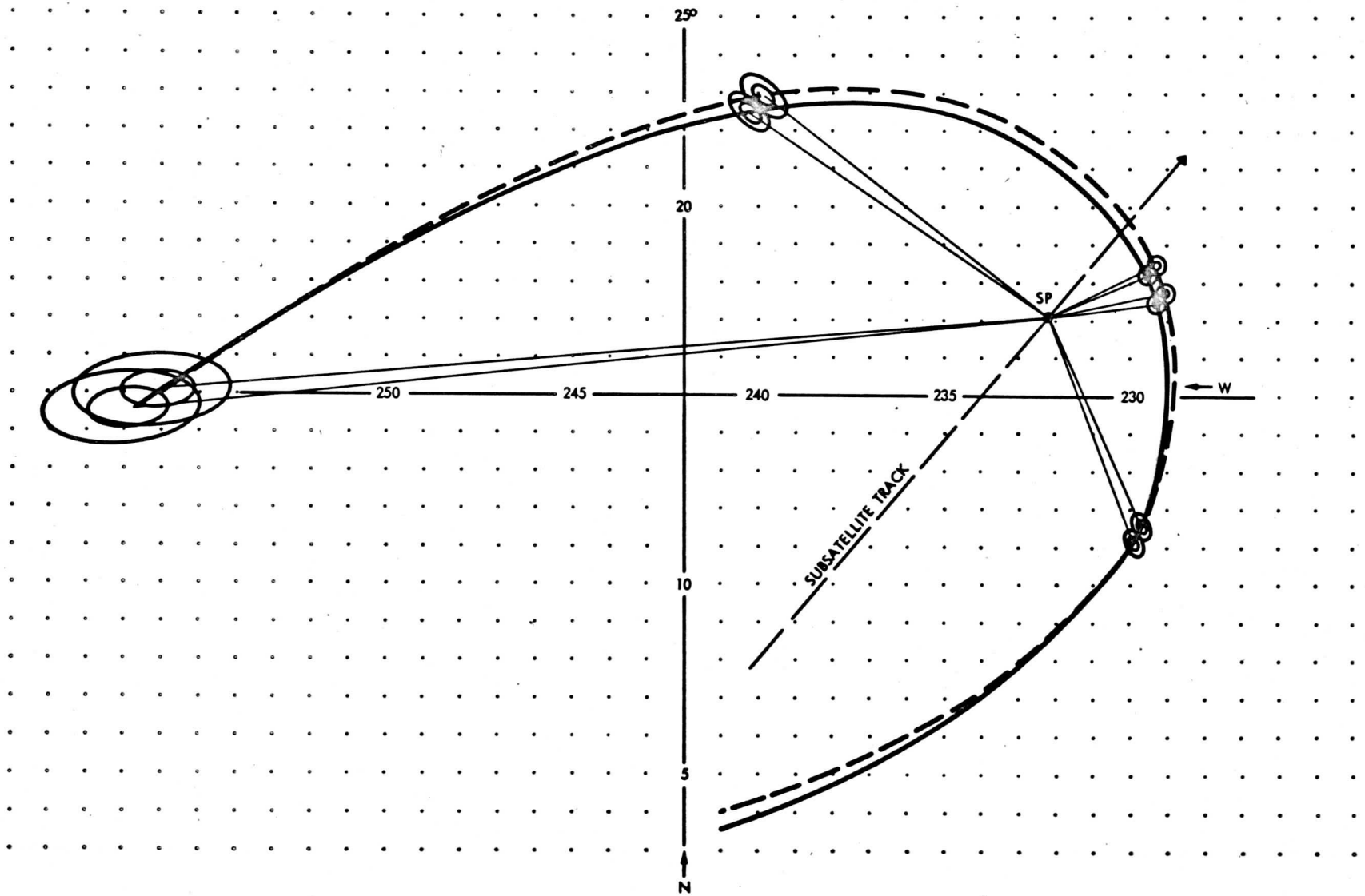
25°
20
SP
250
245
240
235
230
W
SUBSATELLITE TRACK
10
5
N

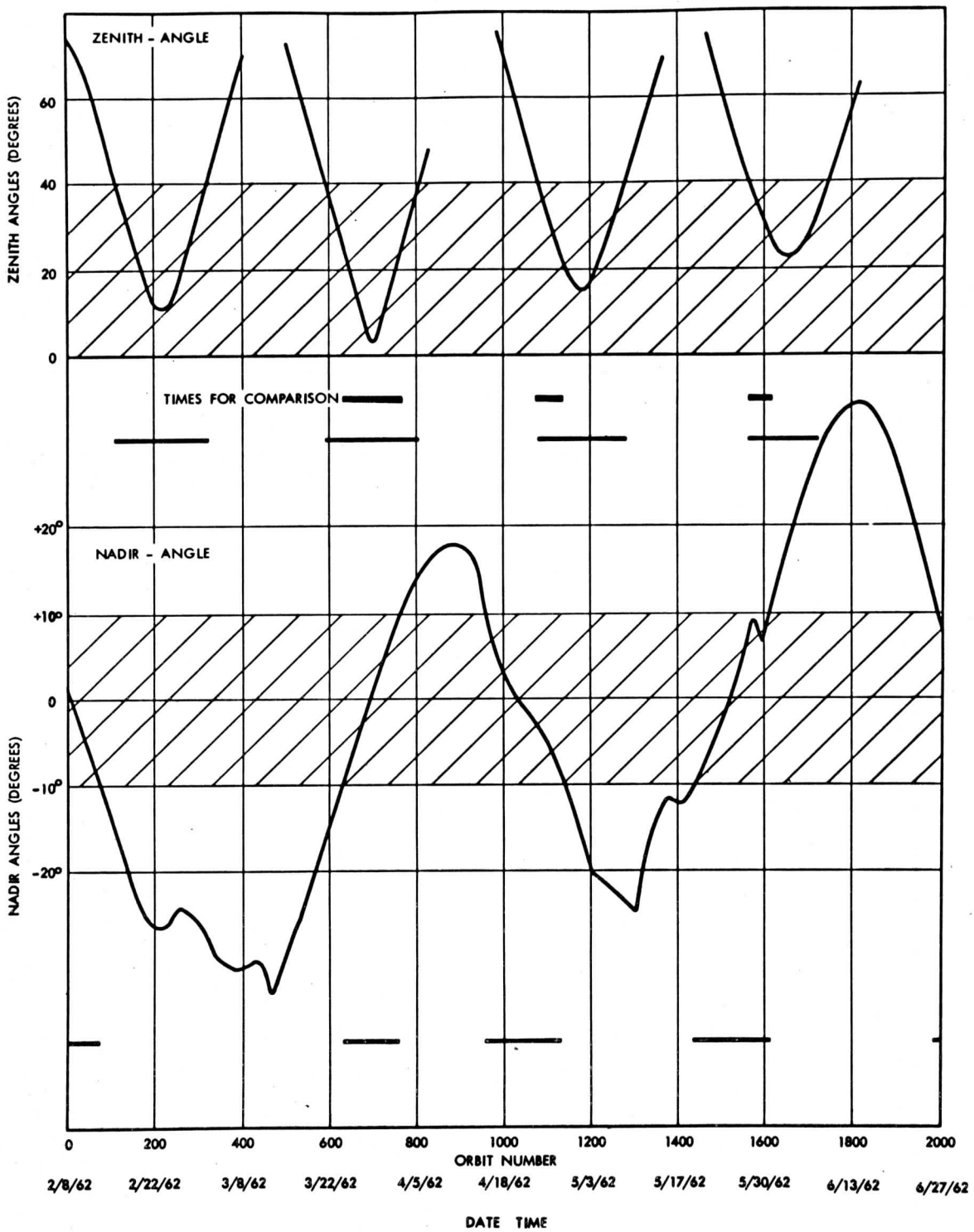
ZENITH - ANGLE
ZENITH ANGLES (DEGREES)
60
40
20
0
TIMES FOR COMPARISON
+20°
NADIR - ANGLE
+10°
0
-10°
-20°
NADIR ANGLES (DEGREES)
0
200
400
600
800
1000
1200
1400
1600
1800
2000
ORBIT NUMBER
2/8/62
2/22/62
3/8/62
3/22/62
4/5/62
4/18/62
5/3/62
5/17/62
5/30/62
6/13/62
6/27/62
DATE TIME

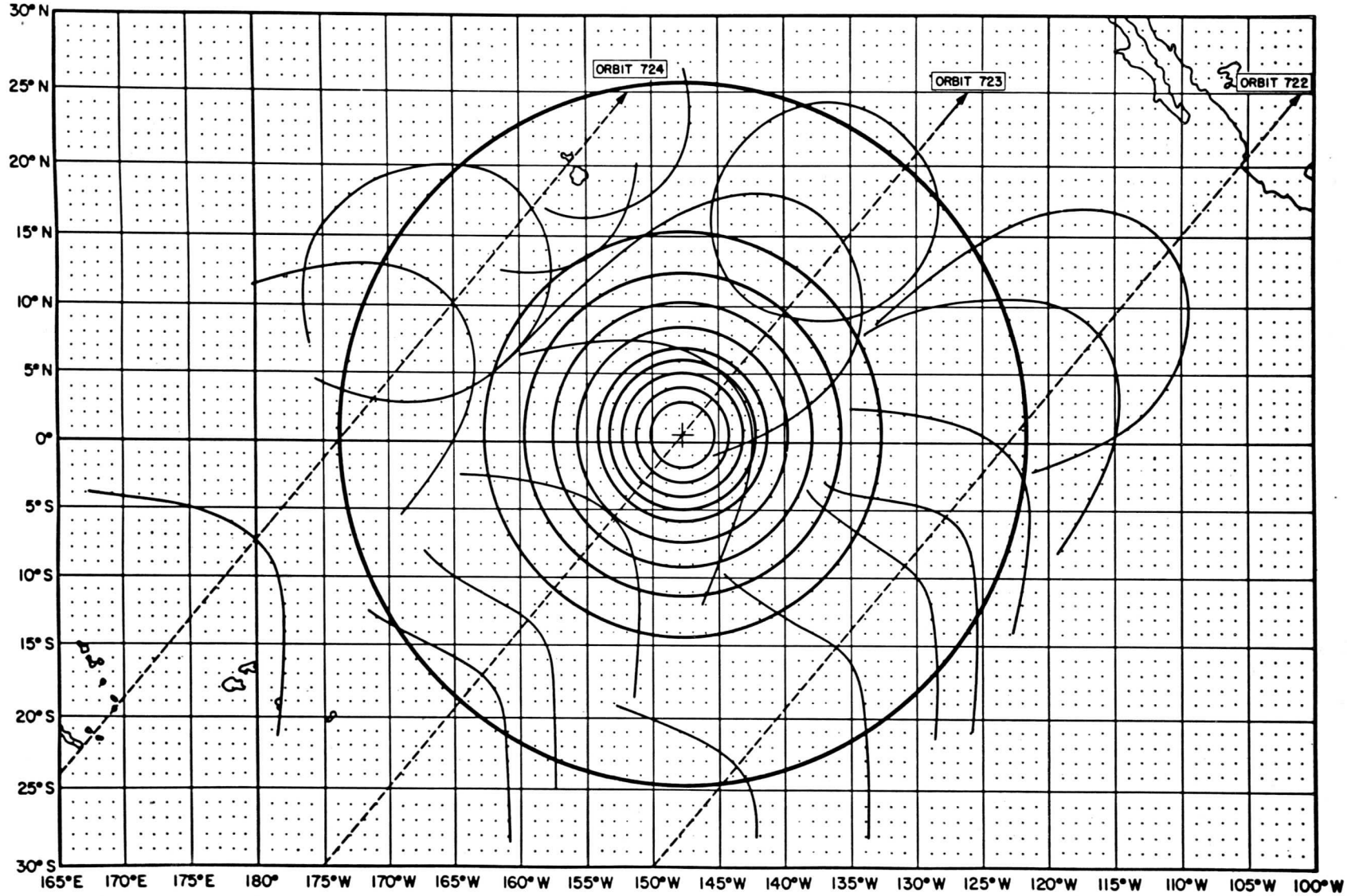
ORBIT 724
ORBIT 723
ORBIT 722
30° N
25° N
20° N
15° N
10° N
5° N
0°
5° S
10° S
15° S
20° S
25° S
30° S
165°E
170°E
175°E
180°
175°W
170°W
165°W
160°W
155°W
150°W
145°W
140°W
135°W
130°W
125°W
120°W
115°W
110°W
105°W
100°W

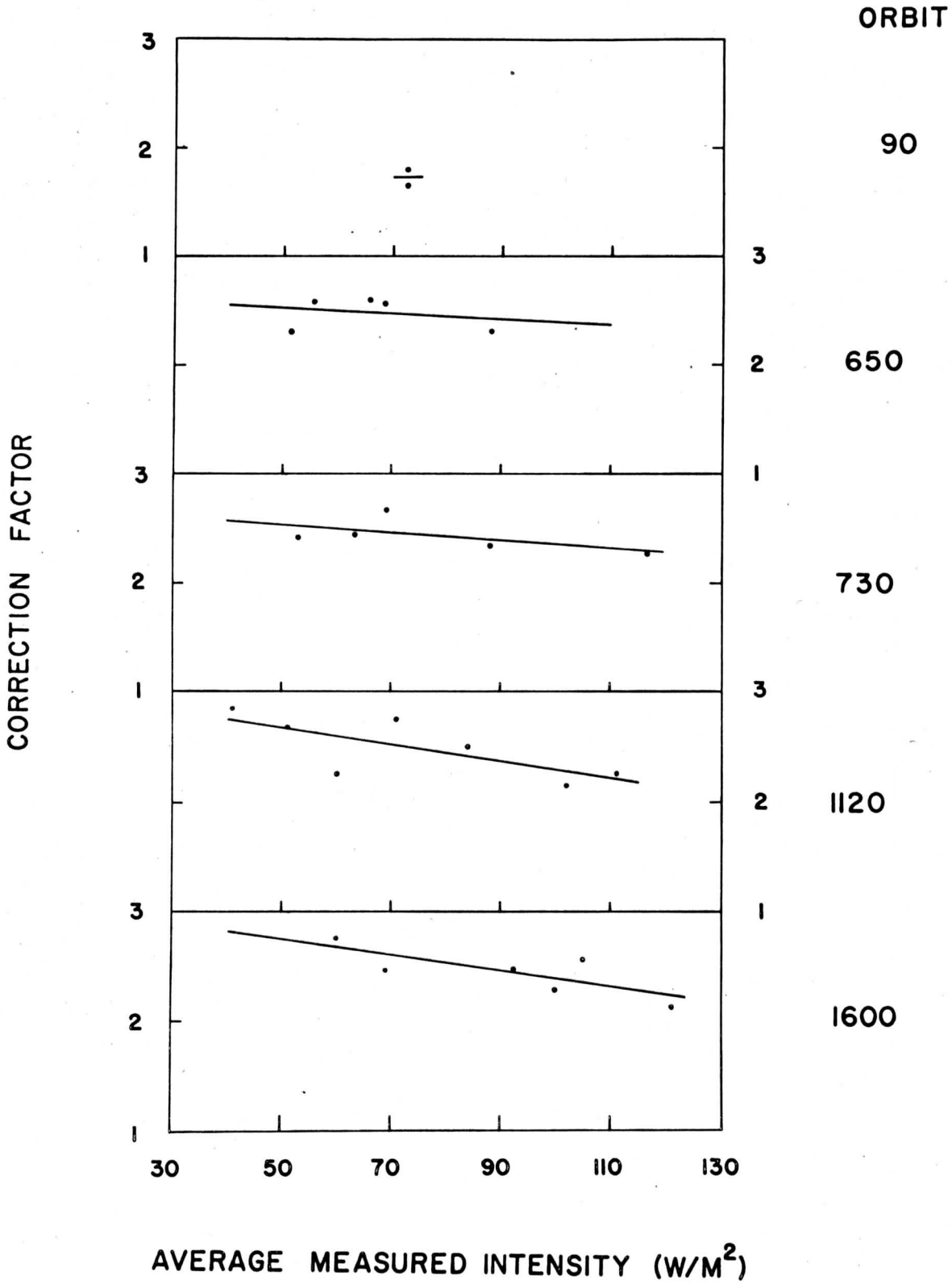
ORBIT
90
650
730
1120
1600
CORRECTION FACTOR
AVERAGE MEASURED INTENSITY (W/M^2)
30
50
70
90
110
130
1
2
3

Figure 7

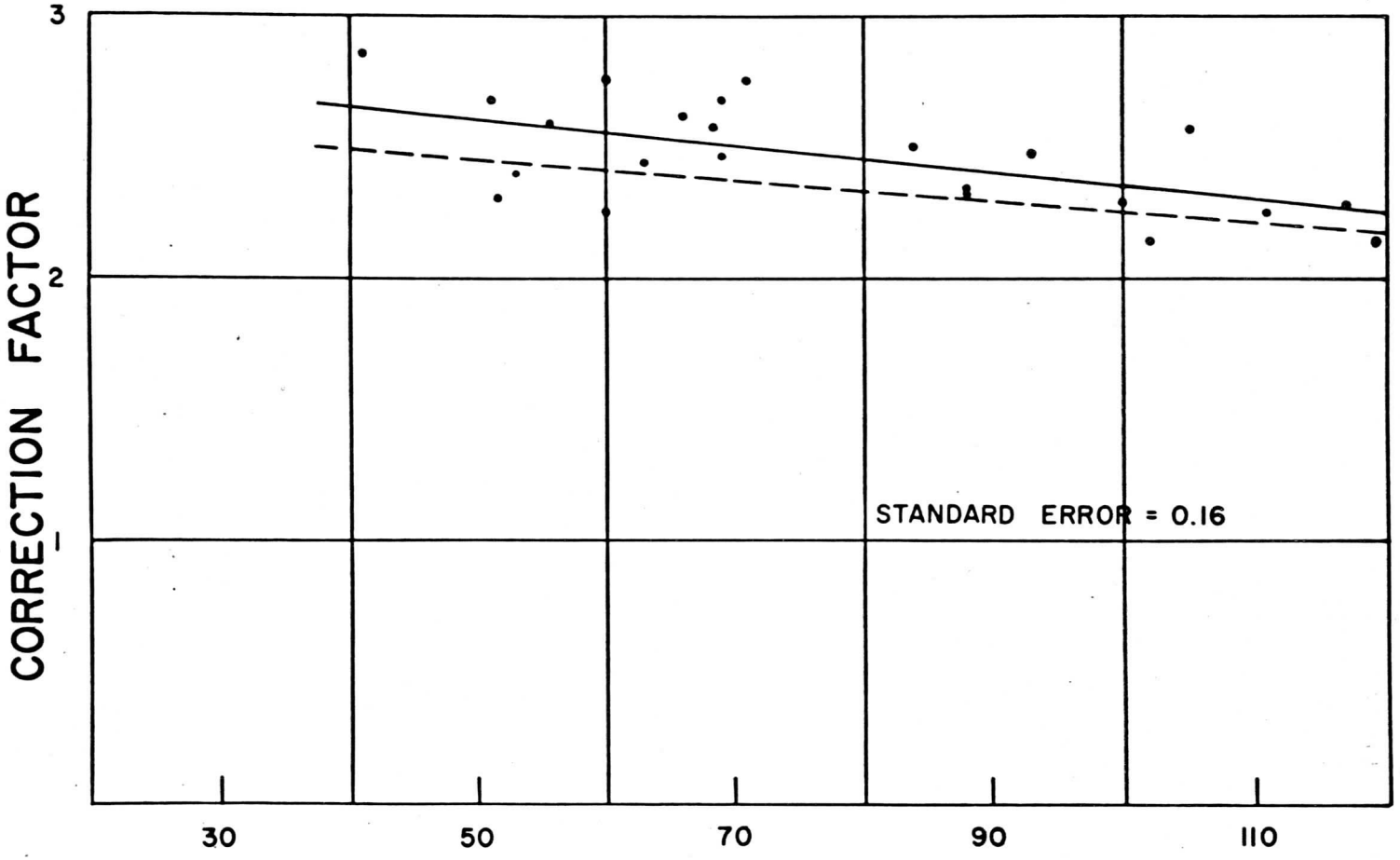
3
2
1
CORRECTION FACTOR
STANDARD ERROR = 0.16
30
50
70
90
110
MEASURED AVERAGE INTENSITY (W/M²)

Figure 8

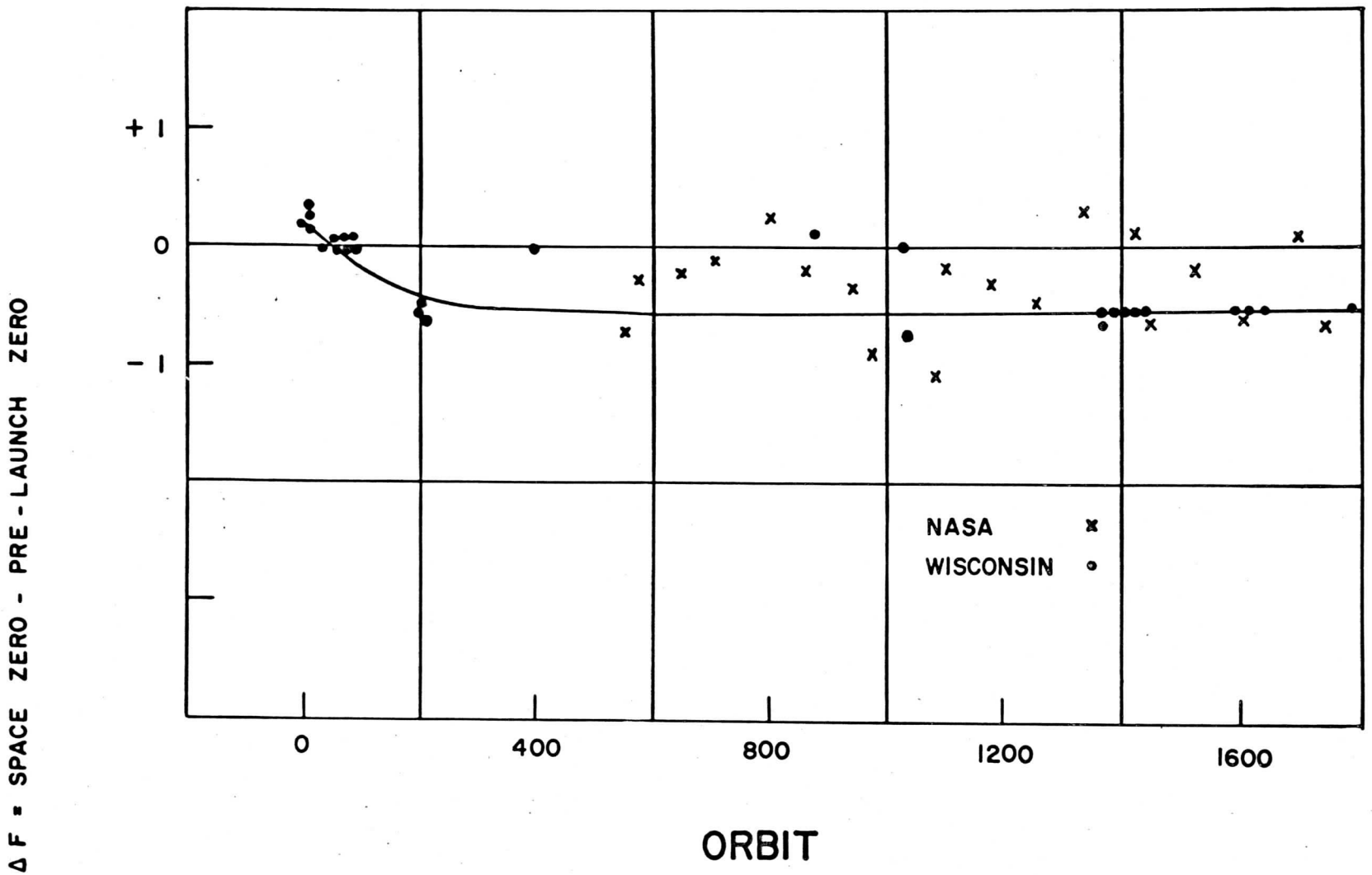
ΔF = SPACE ZERO - PRE-LAUNCH ZERO
+1
0
-1
0
400
800
1200
1600
ORBIT
NASA
WISCONSIN

Figure 9

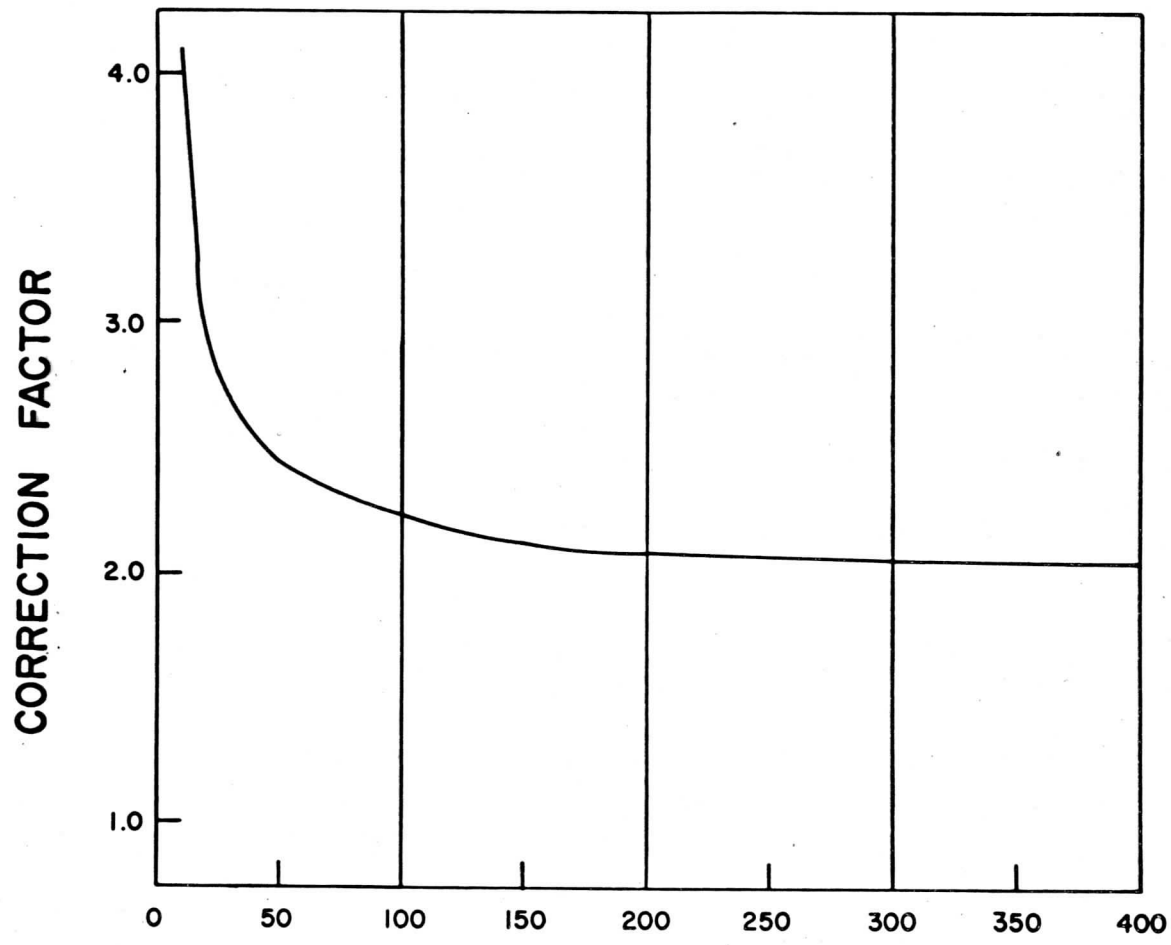
CORRECTION FACTOR
4.0
3.0
2.0
1.0
0
50
100
150
200
250
300
350
400
CHANNEL 3 INTENSITY (W/M²)

Figure 10

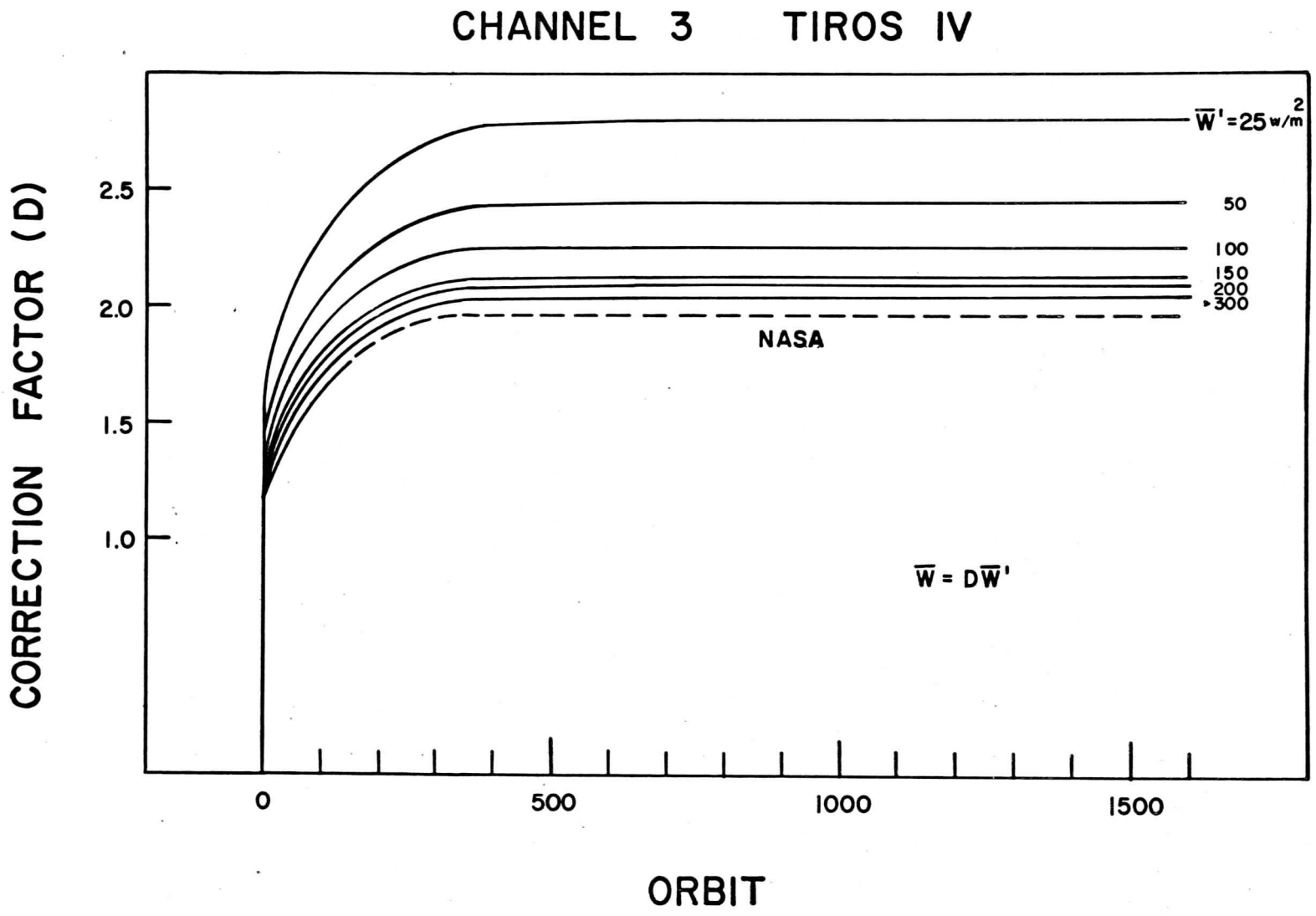
CHANNEL 3 TIROS IV
CORRECTION FACTOR (D)
2.5
2.0
1.5
1.0
$\overline{W}'$=25 w/m^2
50
100
150
200
300
NASA
$\overline{W} = D\overline{W}'$
0
500
1000
1500
ORBIT

Figure II